EurJIC
European Journal of Inorganic Chemistry

Minireview
doi.org/10.1002/ejic.202000513

Europe
European Chemical Societies Publishing

Pincer Chemistry | *Very Important Paper* |

The Pincer Platform Beyond Classical Coordination Patterns

Matthias Vogt*[a] and Robert Langer*[a]

Dedicated to Prof. David Milstein on the occasion of his 73rd birthday

Abstract: The pincer platform provides increased stability and often a rigid coordination mode in transition metal complexes that allows for the incorporation of reactive functional groups in the coordination sphere of a metal. Classical coordination patterns in pincer-type complexes were established over the past decades, involving a preferred set of binding sites. In the current review, we discuss pincer-type ligands with remarkable bonding situations and reactivity patterns, which are beyond the privileged ligand systems frequently used in homogeneous catalysis and bond activation reactions. This includes ligands with ligating atoms based on metalloid elements, π-systems as well as different kinds of metallo-ligands. We categorize the discussed pincer-type ligands herein according to the covalent bond classification and distinguish between metallo-ligands and ligands, which are based on nonmetal and metalloid elements.

1. Introduction

Pincer-type complexes are known for decades and since then they attracted widespread attention with publications of numerous milestones in organometallic chemistry and homogeneous catalysis. These complexes are defined by the meridional coordination of a tridentate ligand to a central metal atom (Figure 1). The rigid environment of these chelating ligands has led to numerous applications in homogeneous catalysis, allows for unprecedented bond activation reactions, as well as for the binding of labile groups.[1–10] Important examples, for instance, involve the first C–C-bond activation,[11] the isolation of a σ-methane complex[12] and the development of templated catalysis.[13,14]

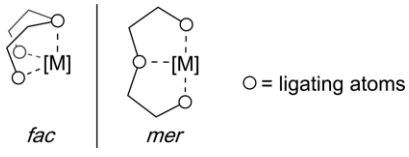

Figure 1. Facial (*fac*) and meridional (*mer*) coordination modes of tridentate ligands. Dotted lines are used for the metal-ligand bond to indicate different types of interactions.

[a] *Dr. M. Vogt, Prof. Dr. R. Langer*
Institute of Chemistry, Faculty of Natural Science II, Martin Luther University Halle-Wittenberg,
Kurt-Mothes-Str. 2, 06120 Halle (Saale), Germany
E-mail: robert.langer@chemie.uni-halle.de
matthias.vogt@chemie.uni-halle.de
https://www.chemie.uni-halle.de/bereiche_der_chemie/anorganische_chemie/33619_3267913/
ORCID(s) from the author(s) for this article is/are available on the WWW under https://doi.org/10.1002/ejic.202000513.
© 2020 The Authors. European Journal of Inorganic Chemistry published by Wiley-VCH GmbH • This is an open access article under the terms of the Creative Commons Attribution License, which permits use, distribution and reproduction in any medium, provided the original work is properly cited.
Part of the German Chemical Society ADUC Prizewinner Collection

Matthias Vogt studied chemistry at the Technical University of Berlin. For his PhD studies, he moved to the ETH Zürich, Switzerland and received his doctorate degree in 2011. He then joined the group of Prof. David Milstein as a postdoctoral fellow at the Weizmann Institute of Science, Israel. In 2014, he started as senior research fellow at the University of Bremen. Since 2020 he holds a position as research associate at the Martin Luther University Halle-Wittenberg, Germany.

Robert Langer is professor for coordination chemistry at the Martin Luther University Halle-Wittenberg. He received his PhD at the University Karlsruhe (TH) in 2009. After a postdoctoral stay at the Weizmann Institute of Science (Israel), he started his independent career at the department of chemistry at the Philipps-University Marburg in 2011. Since 2020, he is a Heisenberg-professor at the Martin Luther University Halle-Wittenberg, Germany.

© 2020 The Authors. European Journal of Inorganic Chemistry published by Wiley-VCH GmbH

Organometallic complexes containing tridentate ligands with a preference for a meridional coordination are known since the 1970s[15,16] and the first definition of the term pincer type ligand by van Koten in 1989 referred to meridionally coordinated tri-dentate ligands with a central anionic carbon-based group and two neutral terminal donor groups.[17] This original definition was subsequently extended to meridionally coordinated ligands with variable number of neutral and anionic binding sites (Figure 1) and until now pincer ligands are often defined by their neutral or anionic binding donor groups.[18]

In recent years, unexpected donor groups, electron accepting groups and even metal fragments were successfully used in such meridional arrangements around a central metal atom for various applications, including the activation of strong bonds and homogeneous catalysis, exemplified, for instance in (de)hydrogenations with relevance for novel atom-economic environmentally benign reaction pathways.[6,9]

While their enormous potential is frequently highlighted in review articles, we want to focus in the current review on ligands from the most common classes according to the covalent bond classification (CBC) with less common binding motifs and intriguing bonding situations. We will show that it is necessary to extent our current view on pincer-type ligands by inclusion of different types of interactions between the metal center and the pincer moiety.

1.1. The Covalent Bond Classification

The covalent bond classification (CBC) originally introduced by Malcom Green distinguishes between different ligand types by formal cleavage of the metal ligand bond into neutral ligand fragments. Using this formalism, the need to define formal oxidation states is obviated and the ligands are categorized into three classes by their neutral form (Figure 2). In addition to ligands forming regular covalent bonds, formally serving as one electron donor (X-type), the two different possibilities for dative covalent bonds by either an electron-donating (L-type) or an electron-accepting (Z-type) ligand are classified.

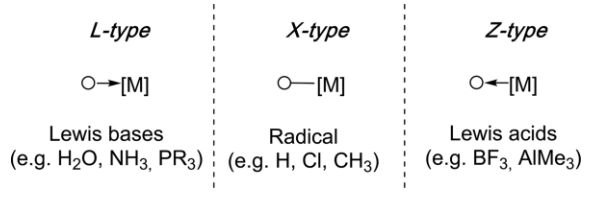

Figure 2. Ligand types according to the covalent bond classification (CBC) and the resulting neutral ligand fragments.

For more detailed insights into the covalent bond classification and their application to coordination compounds we would like to refer to a number of excellent reviews and book chapters.[19–21]

1.2. Abbreviation of Pincer-Type Ligands

In most cases, pincer-type ligands are briefly described by the symbols of their ligating atoms. The coordinated ligand in Figure 3 would accordingly be described as PNP-type pincer ligand. This ligand is linked to the central metal atom by the two terminal phosphino-groups (P) and the central amine group (N). Using this nomenclature, in this review we will discriminate between L-, X- and Z- functions, as well as metal-based ligands that do not fit into the CBC scheme.

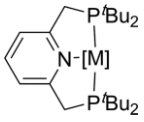

Figure 3. Example of an PNP-type pincer complex.

2. Coordination Patterns with Non-Metal Ligating Atoms

The most common pincer-type ligands are undoubtedly monoanionic (LXL-type) and neutral (LLL-type) with terminal tertiary phosphino-groups and central heteroatom-based donor groups, heterocycle- or aryl-moieties. In the following chapter we will first discuss less common classes of pincer-type ligands and then continue to discuss unusual examples of pincer-type complexes of the more common classes in this context. PEP-type pincer complexes are known for the majority of group 13, 14, 15 and 16 elements (E), and in particular the heavier homologues exhibit some unusual behavior and binding properties. For example, antimony-based pincer-type ligand displayed some coordinative non-innocence, in which, depending on the bound substituents, different ligand functions are observed.[22–25] In the current review, we focus on ligands based on group 13 elements, for which all functions according to the covalent bond classification can be observed, while typical ligating atoms like carbon or nitrogen usually give rise to either X- or L-type function.

2.1. σ-Accepting/Z-Type Binding Sites in Pincer-Type Ligands

As pointed out in the previous section, a dative covalent bond between an electron-deficient compound or Lewis acid and a transition metal complex can be formed (Z-type). Early examples of an unsupported Z-type coordination involve the bent binding of SO_2,[26] while the Z-type coordination of a borane moiety was realized for the first time in scorpionate complexes via B–H-oxidative addition of the bridge-head 30 years later.[27] Subsequently, Z-type ligands based on the element boron were incorporated in pincer-type complexes,[28–42] and used as catalysts in reactions like (de)hydrogenations.[34,38,43–45]

In many cases Z-type ligands are located on an edge or a face of the coordination polyhedron formed by X- and L-type ligands. In consequence, different coordination modes and numbers can be observed in these complexes. In case of the aryl borane moieties different binding modes can even be realized. For example the T-shaped palladium(0) complex **1**[35] clearly contains a boron-based Z-type ligand, while in the related nickel(0) complex **2** an η^3-coordination of the phenyl-bor-

© 2020 The Authors. European Journal of Inorganic Chemistry published by Wiley-VCH GmbH

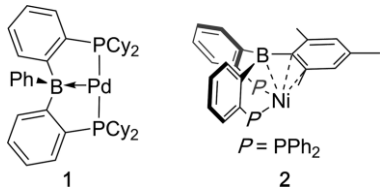

Figure 4. Examples of Z-type complexes with different binding modes.

ane moiety and hence a clear deviation from the T-shape geometry is observed (Figure 4).[34,46]

The incorporation of a σ-accepting group (Z-type) in a pincer ligand can lead to unusual modes of metal-ligand-cooperativity (MLC) in the activation of substrates. The nickel(0) complex **2** with d^{10} configuration reacts with H_2 or silanes to give an η^1-coordinated hydridoborate and a corresponding hydrido or silyl ligand. In contrast to well-established systems of MLC, where an internal base accepts a proton and a hydrido ligand remains at the central metal atom, a hydride is accepted by the Z-type borane group in **2** and a proton adds to the metal center, which is in line with an overall oxidative addition (Scheme 1).[34,38] This constitutes a distinct difference to "classical" modes of MLC, where a change of the metal oxidation state is avoided.[8]

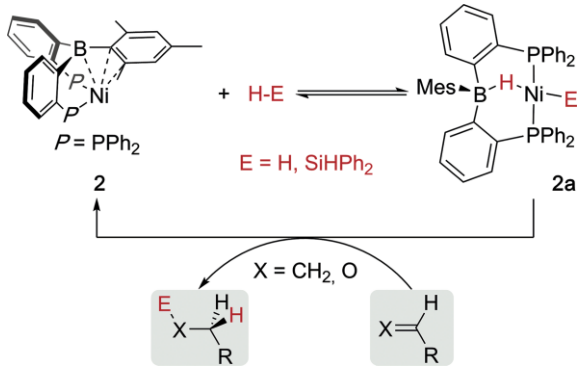

Scheme 1. Activation of H_2 and H_2SiPh_2 by metal-ligand-cooperation of Z-type-based pincer complexes as well as their application in catalytic hydrogenation and hydrosilylation reactions.

Quantum chemical investigations using density functional theory indicate a cooperative mechanism, in which H_2 is heterolytically cleaved across the Ni–B-bond in a concerted step.[39,47] In contrast, for the corresponding palladium(0) complex a stepwise mechanism initiated by oxidative addition of H_2 to the Pd^0 center and subsequent hydride transfer to the Z-type borane was calculated to be the most favored pathway (Scheme 2).[48]

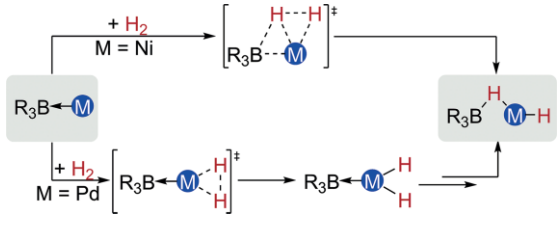

Scheme 2. Simplified pathways for the cleavage of H_2 by Z-type-based pincer complexes.

An unusual mode of allyl acetate activation by the palladium(0) complex **3** was reported by Tauchert and co-workers.[40] In this sequence a formal oxidative addition of the C–O-bond of allyl acetate takes place, the Pd–B-bond is cleaved and the formed acetate is transferred to the borane moiety (Scheme 3). The resulting zwitterionic complex **3a** consists of an anionic but non-coordinating borate group and a cationic fragment with a palladium(II) center coordinated by the two terminal phosphine groups and the generated allyl ligand. Complex **3** was found to be an active catalyst for the allylic substitution of allyl acetate with $HNEt_2$.

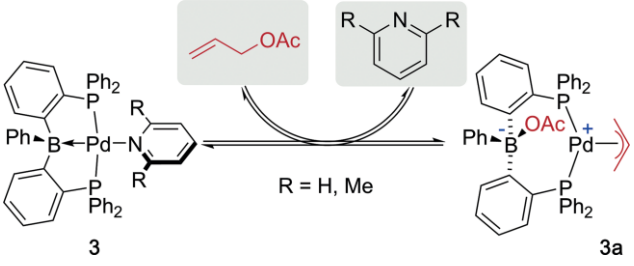

Scheme 3. Cooperative allyl acetate activation by the Z-type-based palladium pincer complex **3**.

Above, we have briefly discussed examples of pincer ligands with a central σ-accepting group based on the element boron. It should be noted that there are ligands with Z-type moieties based on other metalloids, such as silicon, as well as metals.[44] As pointed out in the introduction, we will discuss metallo-ligands in a separate chapter.

2.2. Pincer-Type Ligands Containing X-Type Moieties

Mono- and polydentate X-type ligands of nonmetal elements are very common in classic coordination chemistry and are until now ubiquitous in homogeneous catalysis and organometallic chemistry. Depending on the number of X-type functions in these ligands, a formal heterolytic cleavage would result in mono-, di- or tri-anionic pincer-type ligands. In consequence, the ability to stabilize early transition metals and central metal atoms in high oxidation states increases with increasing charge of these ligands.[49] Such arrangements with pincer-type complexes can lead to unprecedented reactivity patterns and applications in homogeneous catalysis.[50,51] In turn, transition metals in low oxidation states with highly charged ligands are very electron-rich, which can be used to activate very strong bonds under concomitant oxidation of the metal center.

In comparison pincer-type ligands with central X-type functions that are based on metalloid elements, such as silicon and boron, are less explored and show some interesting properties. In particular boron-based pincer-type ligands attracted increased attention after the initial discovery of boryllithium.[52] The pre-ligand **4** includes a borane moiety and can react with a number of transition metal complexes via B–H-oxidative addition to give boryl-based pincer-type complexes (**5**, Scheme 4).[53–60] Depending on the employed metal precursor a sequence of B–H-oxidative addition and H–X-reductive elimination is observed. In either case the presence of a strongly σ-donating boryl group facilitates a number of bond activation reaction and catalytic applications, such as the transfer-de-

© 2020 The Authors. European Journal of Inorganic Chemistry published by Wiley-VCH GmbH

hydrogenation of alkanes,[56,58] the dehydrogenation of dimethylamine-borane[57,61,62] or the hydrogenation and hydrosilylation of olefins.[55,61]

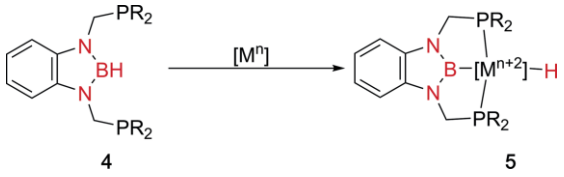

Scheme 4. Formation of boryl-based pincer-type complexes **5** by oxidative addition of the borane **4** (R = alkyl. aryl).

A similar observation was made for triaryl boranes as central moiety in pincer-type ligands (**6**), which are able to react with certain metal complexes via B–C-oxidative addition to the boryl-based pincer complex **7**. Notably, the flexible coordination of the Z-type function, presumably by η^2-coordination, leads to a B–C-oxidative addition and the formation of the X-type-based pincer ligand like in the iridium(III) complex **7** (Scheme 5).[42] Related reactivity was reported by *Tauchert* and co-workers, where the B–C-bond of the phenyl derivative of **6** is cleaved in a palladium(0) complex (**8**) in the presence of aryl iodides. The resulting palladium(II) iodido complex **9** was formed via concomitant C–C-coupling.[63] The boryl group in complex **9** was demonstrated to be Lewis acidic via the coordination of pyridine. In this way the formation of a ligand-stabilized boryl ligand R_2LB^- was achieved (R = anionic aryl substituents, L = neutral substituent such as pyridine).

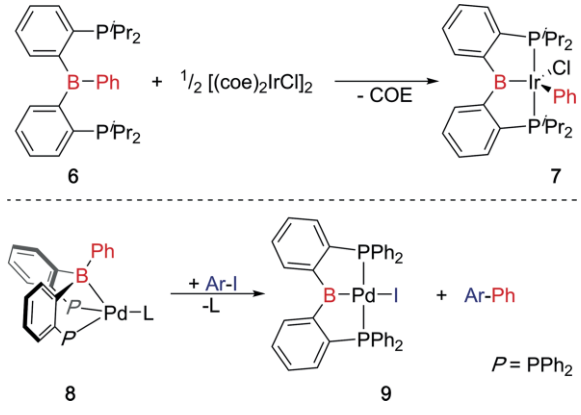

Scheme 5. B–C-bond cleavage of borane moieties in the coordination sphere of transition metals.

The coordination of such strongly σ-donating boryl ligands results in electron-rich transition metal complexes. Quantum chemical investigation of comparable nickel(II) hydrido pincer-type complexes revealed, for instance, that the insertion of CO_2 into the Ni–H-bond is thermodynamically and kinetically favorable for the boryl- and silyl-based complexes.[64]

In most PXP-type pincer ligands, central groups like amido moieties or a dearomatized pyridine scaffold usually act as acceptors for electrophiles in cooperative bond activation, which is a proton in the simplest case. In contrast, a coordinated boryl group can remain Lewis acidic and is therefore more susceptible to the binding of nucleophiles in potential modes of MLC. In this context, the reactivity of the cobalt(I) complex **10** with a boryl-based pincer ligand is worth noting (Scheme 6). This complex readily activates H_2 to give the cobalt(III) dihydrido complex **12** with a borate-based pincer ligand.[61] Complex **10** is a highly active catalyst for the hydrogenation terminal olefins, the dehydrogenation dimethylamino-borane and the transfer-hydrogenation of olefins with dimethylamino-borane. Mechanistic investigations for the hydrogenation of olefins indicate that the hydrido complex **11** with a bridging hydride is the catalytically active intermediate,[62,65] which allows for olefin coordination (**11a**) and subsequent migratory insertion into the Co–H-bond with the bridging hydride (**11b**). Reductive elimination from the resulting cobalt(III) hydrido alkyl species **11b** generates the product alkane and complex **11c**, which readily reacts with H_2 to close the cycle.

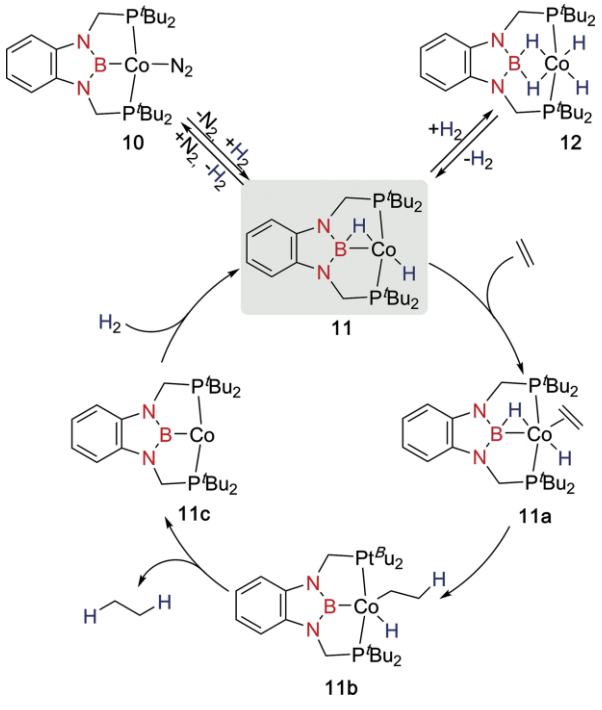

Scheme 6. H_2-activation by the boryl-based cobalt pincer complex **10** as well as the role of the formed catalytic intermediate **11** in the hydrogenation of olefins.

2.3. Neutral Pincer-Type Ligands Containing L-Type Moieties

Pincer ligands with three L-type donor groups are one of the most common class of ligand. Typical examples contain terminal phosphino or carbene groups, as well as neutral donor groups in the central position, such as pyridine or amine groups.[6–9] In the current section we want to highlight pincer-type complexes with unusual central L-type donor groups.

Donor Groups Based on the Element Boron

As shown above, neutral moieties of the type R_3B act as Z-type functions, while coordinated boryl groups $\{R_2B\}^-$ were demonstrated to form ligands of the type $\{LR_2B\}^-$ (X-type), with L= neutral Lewis Base. It becomes evident that the subsequent substitution of anionic by certain neutral substituents allows for

© 2020 The Authors. European Journal of Inorganic Chemistry published by Wiley-VCH GmbH

the stabilization of different kinds of species and ligand types according to the CBC (Figure 5). Using the oxidation state formalism boryl ligands are treated as anionic ligands. However, staying in the picture of the CBC scheme the number of electrons that each neutral ligand contributes to the metal-ligand bonding orbital is counted. The corresponding neutral counterparts, i.e. ligand-stabilized boryl radicals (LR_2B), are known.[66–73] Neutral boron compounds with an occupied p_z-orbital and two stabilizing ligands can be isolated, if σ-donating/π-accepting substituents like cyclic alkylaminocarbenes (CAACs) or carbon monoxide are used.[74–76] The pronounced π-back-bonding in these compounds allows for the stabilization of an occupied p_z-orbital and results in an overall trigonal planar geometry. The nucleophilic nature of such boron compounds is usually demonstrated by the coordination to a transition metal center. These ligands are treated as neutral L-type ligands.

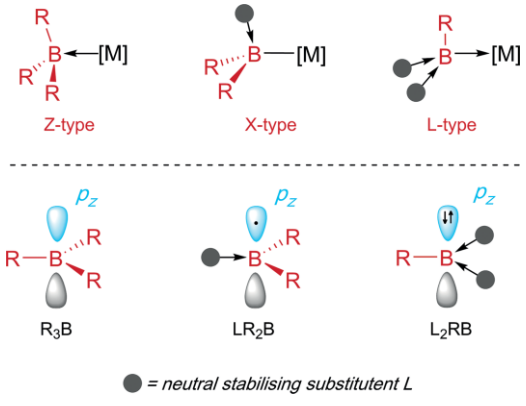

Figure 5. Classification of ligands based on tri-coordinate boron and the corresponding neutral ligand fragments.

However, with more weakly bound substituents and less steric shielding the isolation of these ligand-stabilized borylenes (L_2RB) is often difficult.[77] Nonetheless, transition metal complexes containing neutral donor ligands based on tri-coordinate boron are accessible by B–H-oxidative addition of stabilized boronium salts (**13**, Scheme 7),[78–83] in an analogous way with respect to the oxidative addition of boranes to boryl ligands (Scheme 4). The resulting ligands in complexes of similar to **14** are best described as neutral pincer-type ligands containing three L-type functions.[78,82,84]

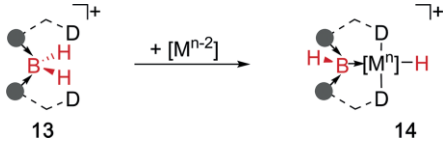

Scheme 7. B–H-oxidative addition of stabilized boronium salts.

Some complexes of type **14** show unique reactivity patterns. For instance, the iron(II) complex **15** is in equilibrium with the iron(0) species **15a**, which is in line with a reversible B–H-reductive elimination/oxidative addition (Scheme 8). Complex **15** can be deprotonated at the Ph_2P-NH-PPh_2 arms, resulting in overall negatively charged pincer ligand via the first deprotonation and a dianionic ligand after the second. Interestingly, the deprotonated complexes exhibit the same reactivity pattern, but the difference in Gibbs energy between the iron(II) und the iron(0) isomer decreases with the degree of "arm deprotonation" and an increasing rate is observed for this equilibrium.[78]

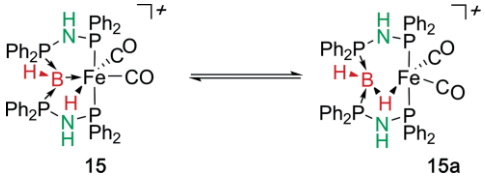

Scheme 8. Reversible B–H-reductive elimination observed for iron complexes.

With relevance to homogeneous catalysis this kind of L-type boron-based ligands were shown to have some interesting properties. For instance, it is well-known that for certain catalytic reactions, such as cross-coupling reactions of inert substrates or olefin metathesis, strongly σ-donating ligands in transition metal catalysts can accelerate these reactions.[85–93] In this context, we have demonstrated for a series of iridium(III) carbonyl pincer complexes with the general formula $[(PXP)IrCl(CO)(H)]^q$ that ligands of the general type $(R_3P)_2BH$ are very strong neutral donors (Figure 6). It was possible to extrapolate the Tolman electronic parameter for monodentate ligands of this $(R_3P)_2BH$ type, using the wavenumber of the C–O-stretching vibration in iridium pincer complexes $[(PXP)IrCl(CO)(H)]^q$ (the group X is in *trans*-position to CO) that can be correlated with known TEP values of the corresponding monodentate derivatives of X. The TEP of a $(R_3P)_2BH$-based ligand was found to be significantly lower than for common spectator ligands in homogeneous catalysts of late transition metals.[82]

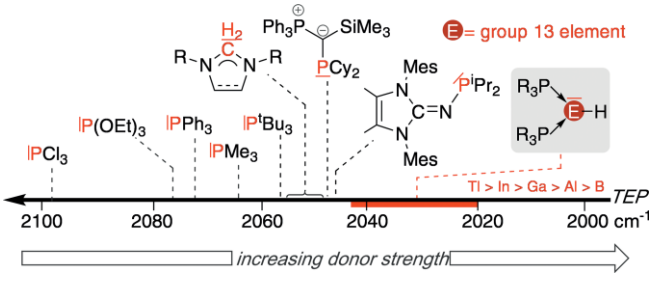

Figure 6. Extrapolated Tolman electronic parameter (TEP) for $(R_3P)_2EH$ (E = B, Al, Ga, In, Tl) in comparison to common electron rich ligands.

Complex **16**, which is a derivative of **15** utilizing CH_2- instead of NH-bridges, is an active catalyst for the dehydrogenation of Me_2NH-BH_3.[83] The reversible B–H-reductive elimination/oxidative addition, shown in Scheme 8, was demonstrated to be an off-cycle equilibrium, which allows for the generation of different, however, catalytically active species (Scheme 9). The iron(II) species (**17**) was shown to operate via a dual-path mechanism involving a deprotonated ligand site. Upon reaction of **17** with Me_2HN-BH_3 the iron(0) complex **17a** is formed, which reacts further with another equivalent of Me_2NH-BH_3 to regenerate **17**, H_2 and half an equivalent of $(Me_2NBH_2)_2$.

Reactivity Patterns in Comparison

Before we continue to highlight other L-type donor groups it is worth to analyze certain elementary steps in organometallic

© 2020 The Authors. European Journal of Inorganic Chemistry published by Wiley-VCH GmbH

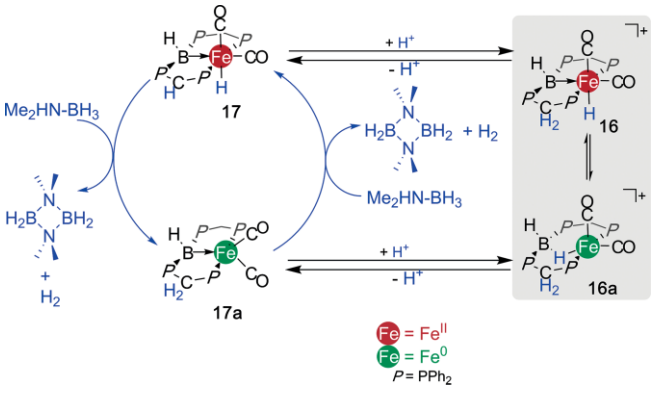

Scheme 9. Simplified mechanism of the acceptorless dehydrogenation of $Me_2NH\text{-}BH_3$, catalysed by iron pincer complex **16**.

chemistry and homogeneous catalysis. The interconversion of complexes with LXL- into LLL-type pincer ligands represents the base for metal-ligand-cooperation (MLC) with transition metal complexes. That is, in these complexes a remote function in the ligand (often the X-type ligand) acts as an internal base necessary for bond activation reactions involving H–X-bonds (H–X = alcohols, amines, etc.).

As shown above, different ligand types with respect to the CBC scheme can be incorporated into pincer ligands based on the element boron. Interestingly, for all ligand types certain reactivity patterns have been reported, leading to the cleavage of the metal boron bond and the formation of a tetra-coordinated boron species, which can be described by the generalized structure **I** (Scheme 10). Depending on the available vacant coordination sites at the central metal atom and the number of B–H-bonds, the cleavage of the metal boron bond either results in a η^1- (**II**, **IV**) or a η^2-coordination (**III**) of B–H-bonds, respectively (Scheme 10). In this context, different pathways can be differentiated for the reversible formation of anionic hydridoborate moieties: (i) The migration of an X-type ligand from boron to the metal center, such as a hydride, is observed to give a pincer complex (**IIa**) with a central Z-type moiety and a hydrido ligand at the metal center. (ii) Reductive elimination and the liberation of two equivalents of H_2 can take place in metal-dihydrido hydridoborate complexes **III**, leading to a boryl-based pincer-type ligand in **IIIa**. Obviously, the preferred reaction pathway depends on the coordinated metal fragment with its ancillary ligands as well as on the substituents at the boron atom. The strong impact of the boron-bound substituents is underlined by the unusual reactivity of diphosphino boronium cations (**IV**), in which two anionic substituents are replaced by neutral phosphine groups. In this case the B–H-oxidative addition of the tetrahedral boron moiety **IV** to **IVa** is observed.

In section 2.1, the flexibility and novel modes of metal ligand cooperation for σ-accepting boron-based groups BR_3 in pincer ligands (Z-type) were discussed. With a view on the neighboring elements in the periodic table carbon and nitrogen, related pincer-type complexes with central ER_3-groups can be identified and it is possible to compare basic elementary steps for these complexes (Scheme 11). In this context, the implementation of such groups in pincer-type complexes allows to compare reactivity patterns.

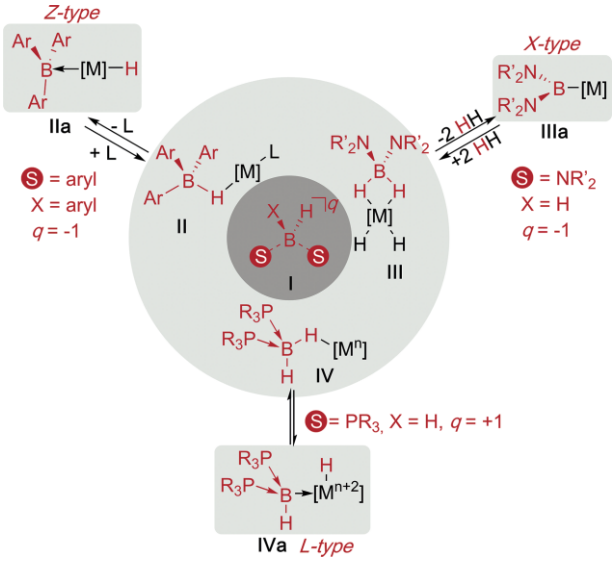

Scheme 10. Simplified reactivity patterns of tetrahedral boron-based ligands, leading to different ligand types according to covalent bond classification (Ar = aryl).

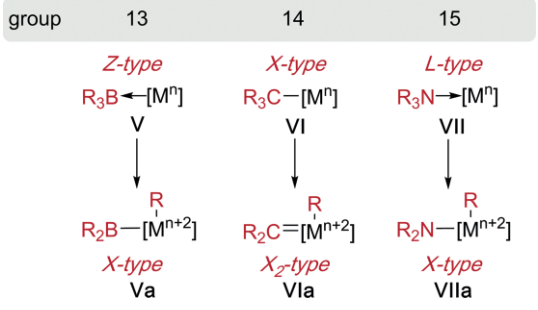

Scheme 11. Elementary steps like the oxidative addition that are observed for coordinated ER_3-groups in in pincer-type complexes (E = B, C, N), leading to different ligand-types.

Secondary and tertiary amines are common ligands and popular donor groups in pincer-type complexes. For example, secondary and tertiary amine-based pincer-type ligands (L-type) were reported to coordinate to rhodium precursors and the resulting complexes (**VII**) subsequently react via intramolecular N–H- or N–C-oxidative addition to amido-based complexes **VIIa** (X-type).[94] Analogous pincer-type ligands with a group 14 element as ligating atom, like in the alkyl-based pincer-type complexes (**VI**) are categorized as X-type. For different transition metal complexes, the deprotonation and formation of alkylidene complexes (**VIa**, X_2-type) was reported.[95–97] As pointed out in Scheme 11, pincer-type complexes (**V**) with a central triarylborane moiety (Z-type) can react via an intramolecular B–C-oxidative addition to the boryl-based (X-type) pincer-type complexes (**Va**).[42,63] In conclusion, it becomes evident that at least in pincer-type complexes, all ligand types according to the CBC scheme Z-, X- and L-type, can undergo an intramolecular E–R-oxidative addition giving rise to either X- or X_2-type groups.

For other elementary steps than oxidative addition and reductive elimination a direct comparison is difficult, as certain co-ligands or groups in ß-position are required and experimen-

© 2020 The Authors. European Journal of Inorganic Chemistry published by Wiley-VCH GmbH

tal precedence is in part missing. However, the ß-hydride elimination of amido-based pincer ligands (**18**) is well documented, leading to a central imine function (L-type) in **19** (Scheme 12).[6,7] Complex **19** can further tautomerize to the corresponding enamine **19a**, which can lead to the liberation of H_2 in the presence of hydrido ligands. For alkyl-based pincer-type complexes like **20** a ß-hydride elimination was observed, as well. The resulting olefin-based pincer-type complexes **21** show some interesting reactivity patterns and fairly flexible binding but are much less investigated than the classical PNP- and PCP-type ligands in pincer chemistry. In particular in the context of the covalent bond classification and the resulting different ligand function associated with olefinic binding sites, a detailed analysis of their properties is noteworthy and given below.

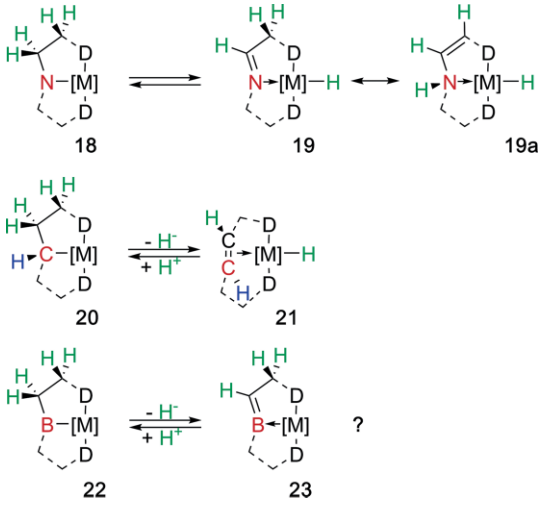

Scheme 12. Possible and hypothetical ß-hydride elimination of from X-type-based pincer ligands in comparison.

So far, boryl-based pincer-type complexes with ß-hydrogen atoms (**22**) are unprecedented, but the ß-hydride elimination from such species would lead to an alkylidene borane (**23**), which were reported to act as olefinic ligands as well as Lewis acids,[98] which in consequence should be able to act as Z-type ligands, as well. It should be noted that Owen and co-workers recently reported an η^2-coordinated alkylidene borane.[99]

Pincer Ligands Incorporating Olefinic Binding Sites

Owing to their unique binding features olefins are an intriguing class of ligands, which were also utilized as steering ligands exceeding their sole function as labile placeholders.[100,101] In general, coordinated to a metal center, olefins can offer a two-fold synergistic binding mode. That is, the metal can bind via an empty d_σ orbital and the π-electron system to form a σ-bond and further π-backdonation from the metal into π^* orbital of the olefin gives rise to π-bonding. As a result of the latter, the C=C-bond is lengthened due to population of the π^* anti-bonding orbitals. This dual binding scheme (Dewar-Chat-Duncanson model)[102] gives rise to two resonance structures resembling different CBC ligand types: Sole σ-donation results in an L-type ligand (Figure 7-I), whereas strong π-back bonding gives rise to a metalla-cyclopropane motif resembling an X_2-type ligand (Figure 7-I).[20,101] However, in the here presented examples we want to relate to the η^2-bonded olefins in the pincer ligands as L-type ligands as their main bonding feature and categorize them accordingly. In terms of olefinic pyridine-based pincer-type complexes *Sacco*, *Vasapollo* and co-workers describe in two early reports 2,6-diallylpyridine (= DAP, Figure 7-II, **24**), which was coordinated to Rh, Ir, Ru, Pd, and Pt metal centers. Structural evidence of olefin-pyridine-olefin pincer-type binding was given for $[Ru(DAP)(PPh_3)Cl_2]$ (**27**), in which the Ru resides in the center of a distorted octahedral geometry with the tridentate DAP ligand coordinated in a meridional fashion. However, the DAP ligand is readily exchanged upon reaction with CO.[103,104] Surprisingly, a literature search revealed that the DAP ligand platform has not been widely explored.

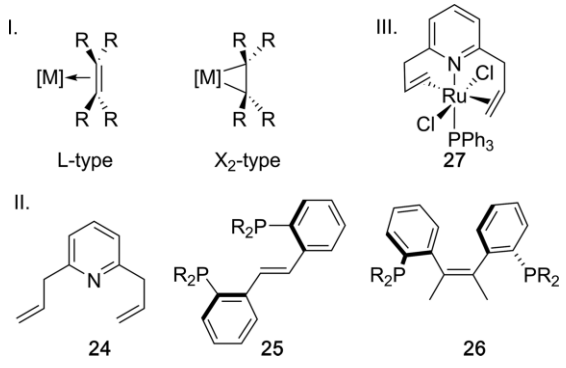

Figure 7. I. Resonance structure of olefin complexes. **II**. Prominent olefin-, pincer-type ligands. **III.** Structurally characterized DAP complex.

Internal alkenes substituted with two phosphine donors were shown to be suitable platforms for pincer-type ligands, however, the examples reported are not numerous. For instance, *trans*-stilbenes decorated with two 2,2′-bis(diphenylphosphino)-functions were mentioned in early reports by *Bennett* and co-workers (Figure 7-II, **25**).[105–107] The two P-donors of such P-olefin-P ligands can occupy mutual *trans*-positions upon coordination to metal fragments with octahedral or square-planar coordination spheres, thus inflicting metal interactions with the central olefin and giving rise to a κ^3-coordination in a meridional LLL pincer ligand motif. Iluc and co-workers explored a range of transition metals coordinated to the 2,2′-bis(diisopropylphosphino)-*trans*-stilbene *t*P*i*PrCH=CHP*i*Pr (ligand **25-***i*Pr Figure 7-II, R = *i*Pr) in a meridional pincer-fashion with examples comprising group 10[108,109] and group 9 and coinage metals.[110] A strong feature of 2,2′-bisphosphino *trans*-stilbene pincer ligands is their potential ability to stabilize various oxidation states of the metal centers associated with their ability to accommodate various coordination spheres. For instance Iluc and co-workers describe a series of Ni compounds in the formal oxidation state 0 +I and +II associated with trigonal planar, tetrahedral, and square-planar coordination geometries, respectively (Scheme 13).[108] Specifically, the reaction of 2,2′-bis(diisopropylphosphino)-*trans*-stilbene and $[Ni(cod)_2]$ in THF gives rise to the Ni^0 compound [Ni(*t*P*i*PrCH=CHP*i*Pr)] (**28**) with pseudo-trigonal geometry. The olefin is η^2-bound to the Ni^0 center with a deviation of only 29° from the plane defined by the two phosphorus atoms and the nickel center. Upon reac-

© 2020 The Authors. European Journal of Inorganic Chemistry published by Wiley-VCH GmbH

tion of **28** with one equiv. MeI the cationic methyl nickel species [Ni(*t*P*i*PrCH=CHP*i*Pr)Me]I (**29**) is formed having a distorted square-planar geometry with the pincer binding via both P-donors and the central η^2-bound olefin in *mer*-configuration. The overall positive charge of the complex is balanced by a non-coordinating iodide ion. Remarkably, the olefin is approaching a perpendicular position with respect to the Ni–P–P plane (deviation of 71°) indicating a rather flexible pincer scaffold. When complex **28** is reacted with 0.5 equivalents of I_2 the neutral complex [Ni(*t*P*i*PrCH=CHP*i*Pr)I] (**30**) is formed**.** The complex entails a nickel center in the formal oxidation state of +I residing in a distorted tetrahedral coordination sphere.

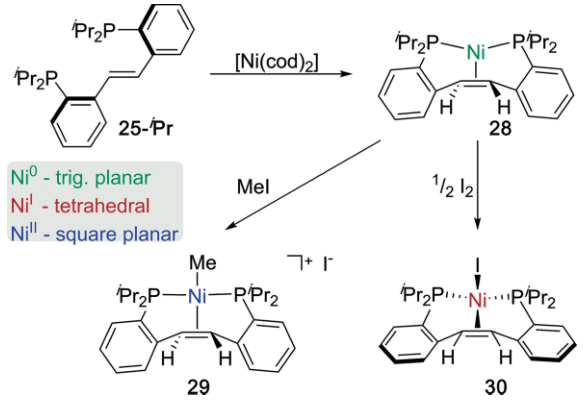

Scheme 13. tP*i*PrCH=CHP*i*Pr-based nickel pincer complexes: Preparation of a compound series of Ni^0, Ni^I, Ni^{II}.

Interestingly, also η^2-coordination of a *cis*-olefin in a stilbene reminiscent P-olefin-P pincer ligand was shown by Iluc in a tris-coordinated Pd^0 complex [Pd(*cis*PCMe=CMeP)] with a (Z)-2,3-bis(2-diisopropylphosphinephenyl)-2-butene ligand (Figure 7, **26**).[109]

Another feature of 2,2′-bisphosphino *trans*-stilbene pincer ligands is their potential hemilabile binding of the central olefin. As mentioned above Iluc and co-workers describe a series of transition metal complexes (Fe, Co, Rh, Cu, and Ag) featuring the *t*P*i*PrCH=CHP*i*Pr pincer-ligand **25-***i*Pr. Depending on the metal type and the oxidation state, the pincer ligand **25-***i*Pr clearly shows hemilabile bonding features. This was well demonstrated for a series of neutral and cationic cobalt compounds in the formal oxidation state of +I and +II (Scheme 14).[110] Reaction of **25-***i*Pr with $CoCl_2$ gave the tetrahedral complex [Co(κ^2-*t*P*i*PrCH=CHP*i*Pr)Cl_2] (**31**), in which the κ^2–coordinated ligand **25-***i*Pr binds exclusively via both phosphine donors to the Co^{II} center. Upon chloride abstraction, the formation of [Co(*t*P*i*PrCH=CHP*i*Pr)Cl]BArF (**32**) was observed. The formation of the new cationic species was accompanied by olefin η^2-coordination and a transformation to a pseudo square-planar geometry. Upon one-electron reduction of complex **31** the authors report the formation of the neutral complex [Co(*t*P*i*PrCH=CHP*i*Pr)Cl] (**33**). The compound has a Co center in the formal oxidation state of +I residing in a pseudo-square-planar coordination sphere. Remarkably, reaction with CO did not lead to dissociation of the olefin, instead the complex increased its coordination number and the trigonal bipyramidal [Co(*t*P*i*PrCH=CHP*i*Pr)(CO)Cl] (**34**) was formed suggesting strong bonding of the olefin in Co^I complexes in this series. Inspection of the C=C interatomic distances (Table 1) reveals an elongation of the olefinic C–C-bond upon reduction of the Co center indicating increased backdonation.

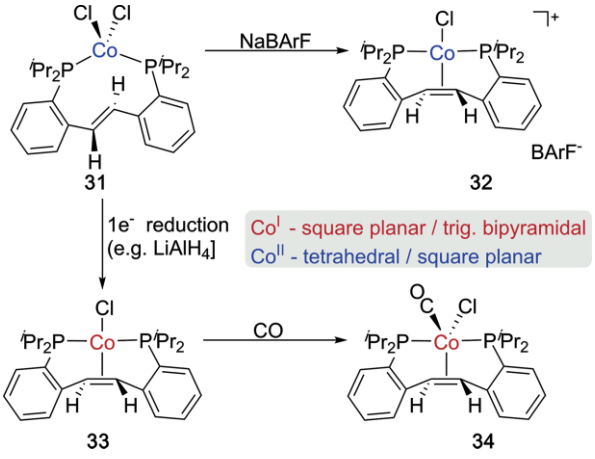

Scheme 14. Cobalt pincer complexes and their reactivity.

Table 1. Geometries and distances in cobalt complexes with olefin-based pincer ligands.

Complex	**31**	**32**	**33**	**34**
Geometry	tetrahedral	square planar	square planar	trigonal bipyramidal
$d_{C=C}$ / Å	1.317(8)	1.397(6)	1.442(9)	1.438(7)

Related R_2P-L-PR_2 pincer systems incorporating a center alkyne moiety are sparsely reported.[111–114] Noteworthy, the group of Agapie has intensively explored complexes decorated with *para*-terphenyl bisphosphine ligands (R_2P-L-PR_2 with L=aryl). This ligand family proved to be cooperative very flexible and redox-active due to the unsaturated and coordinative versatile nature of the pendant central aromatic ring.[115–117]

We have recently reported an olefinic tridentate actor ligand dbap-py (**35**) comprising of a 2-methyl pyridine unit and an azepine component fused by an N-alkylation (Scheme 15),

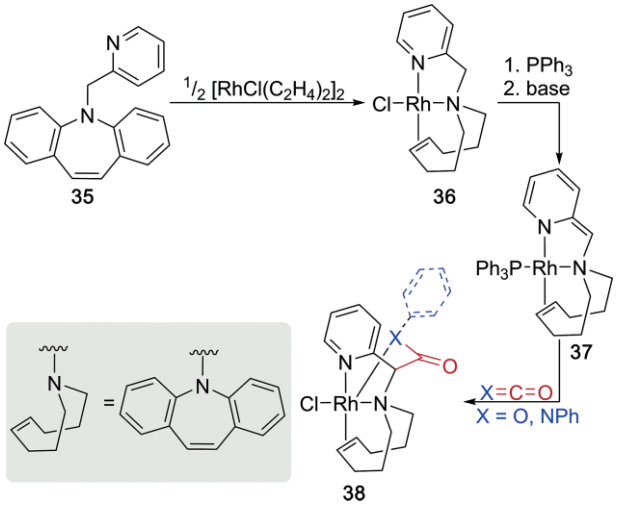

Scheme 15. Cooperative binding of CO_2 and phenyl isocyanate in [Rh(dbap-py*)(PPh_3)].

© 2020 The Authors. European Journal of Inorganic Chemistry published by Wiley-VCH GmbH

which was chelated to a Rh^{I} center (**36**) via the N-donors of the pyridine and azepine unit, as well as via the η^2-coordination of the olefin (N-N-olefin chelation). The ligand scaffold is rather flexible as it can accommodate distorted square planar, as well as trigonal bipyramidal coordination spheres in Rh(I) compounds. The coordinated **35**, however, shows reactivity reminiscent of classical pyridine-based pincer-type complexes. That is, upon deprotonation of the methylene moiety the π-system of the pyridine ring is disrupted ("dearomatization") and a C-nucleophilic methine-group is formed (**37**). Such 'dearomatized' pyridine (pincer) ligands can enable substrate bond activation via metal-ligand cooperation under 'rearomatization' of the pyridine moiety (**38**).[9,118,119] In this context, the cooperative binding of CO_2 has been observed in "classical" pyridine-based pincer complexes.[120–124]

Upon deprotonation, dbap-py* (* denotes the deprotonated ligand) adopts a planar structure and binds the metal center in a meridional fashion. The square-planar coordination sphere in [Rh(dbap-py*)(PPh_3)] (**37**) is completed by an additional PPh_3 ligand. The "dearomatized" complex [Rh(dbap-py*)(PPh_3)] (**37**) reacts indeed metal-ligand cooperatively with the C=O double bond of CO_2 or N=C bond of phenyl isocyanate to give the corresponding κ^1-O carboxylate or κ^1-N amidate, respectively, under C–C and Rh–O/N bond formation and concurrent "rearomatization" of the pyridine ring (Scheme 15). Remarkably, MLC in this particular case allowed for the convenient access to an unprecedented κ^1-N amidate motif in Rh(I) complexes (Scheme 15, **38**) demonstrating the MLC as powerful tool to generate novel unprecedented structural motifs.[125]

3. Coordination Patterns with Metal-containing Pincer-Type Ligands

Metal-based ligands gained increased attention in recent years, due to their ability for flexible binding and the possibility to enable unprecedented reactivity patterns. Metal ions and atoms can be bound in pre-defined pockets of polydentate ligands, which are able to react with a transition metals with formation of a metal–metal-bond. The resulting multinuclear complexes can in part be analyzed according to the covalent bond classification, which allows to distinguish between Z-, X- and L-type metallo-ligands.

3.1. Covalently Linked Metal-Based Pincer-Type Ligands

Lewis-Acidic Metallo-Ligands

The borane-based ligand **6** reacts with transition metal precursors like [AuCl(SMe_2)] to the pincer-type complex **40**,[29] in which the central borane moiety functions as a Z-type ligand as described in section 2.1. The same reaction with analogous ligands of the heavier homologues (**39a** and **39b**) leads to different results: The aluminum-based ligand **39a** gives rise to a zwitterionic species (**41a**), in which the chlorido ligand of the gold precursor was transferred to the aluminum, leaving a tetrahedral aluminate scaffold and a cationic gold phosphine complex with a linear geometry.[126] The related gallium-based ligand **39b** yields a mixture of the zwitterionic complex **42a** and the Z-type-based pincer complex **42b** in solution, which were found to be in equilibrium.[127] Quantum chemical investigations revealed that regardless of the substituent R in the ligand shown in Scheme 16, the zwitterionic gold complex was found to be more stable for all aluminum-based ligands, while the complexes with a Z-type pincer ligand are calculated to be the most stable isomer for all boron-based ligands.[126]

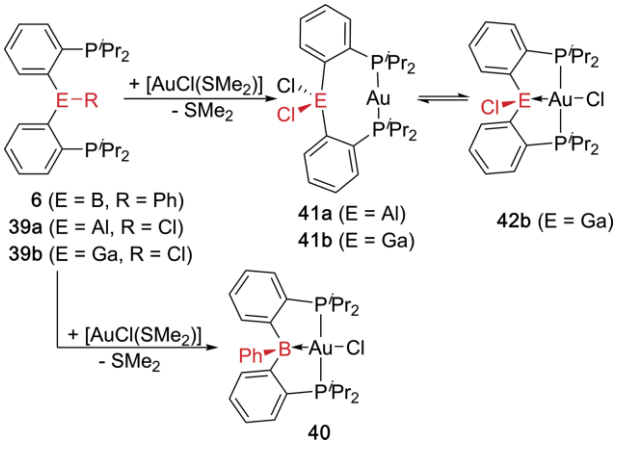

Scheme 16. Comparison of the coordination behavior towards [AuCl(SMe_2)] of boron-, aluminum- and gallium-based ligands.

Further examples of pincer-type ligands containing a central Lewis-acidic ligand site, were reported by Tauchert and coworkers. Using a predefined pocket Li^+-, Cu^+- and Zn^{2+}-based ligands were used to prepare palladium and rhodium complexes (**42–44**, Figure 8).[128,129] In this case, the positive charge of the metallo-ligand makes a meaningful application of the covalent bond classification challenging, as the formal cleavage into neutral ligand fragments would lead to radicals (X-type) in case of lithium and copper, and a neutral two electron donor (L-type) in case of zinc.

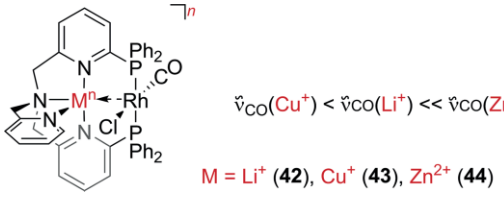

Figure 8. Rhodium carbonyl complexes with Lewis-acidic metallo-ligands.

A series of rhodium chloride carbonyl complexes with these ligands (**42–44**) revealed that the charge of the central metallo-ligand seems to have the strongest impact on the measured wavenumber of the C-O-stretching vibration, which in turn usually represents a qualitative measure for the electron-richness of the central rhodium atom. Moreover, the rhodium(I) complexes exhibit square-pyramidal geometry, suggesting the coordination of a Lewis-acidic or Z-type ligand.

Anionic Metallo-Ligands

The formation of a number of aluminum-based metallo-ligands, in which the central aluminum moiety is formally categorized as an X-type function (e.g. **45**, Scheme 17), was reported to be

© 2020 The Authors. European Journal of Inorganic Chemistry published by Wiley-VCH GmbH

obtained via reduction of the corresponding Z-type ligands.[130,131] An alternative approach involves the Al-H oxidative addition of corresponding alanes, similar to the boron compound **4**.[132] In agreement with the classification for boron in Figure 5 the aluminum-based ligand in **45** may be described as LR_2Al (X-type), but in contrast to the lighter element boron the aluminum center in **45** remains Lewis acidic and allows for the coordination of a second Lewis base (in addition to the present amine group). Accordingly, the *ortho*-metalation of pyridine by complex **45** is observed in the presence of $HSiEt_3$, yielding the rhodium(III) complex **46**.

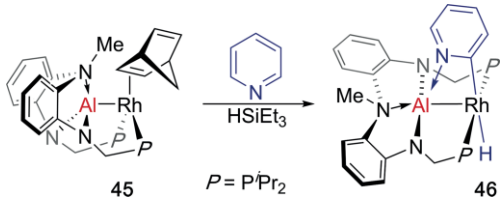

Scheme 17. A group 13-based metallo-ligand, which is considered as X-type function.

Diphenylphosphino-substituted terpyridines selectively bind group 13 halogenides ECl_3 (E = Al, Ga, In) via the pyridine donor groups, yielding the ionic pre-ligand **47** (Scheme 18).[133] This compound readily reacts with the palladium(0) precursor $[Pd_2(dba)_3]$ to give complex **48** encompassing a square-planar coordinated palladium(II) center and a reduced group 13-based ligand. Notably, the complex with the aluminum-based ligands is a competent catalyst for the hydrosilylation of carbon dioxide to formic acid silyl ester, while the complexes with corresponding gallium- and indium-based ligands showed significantly reduced activities.

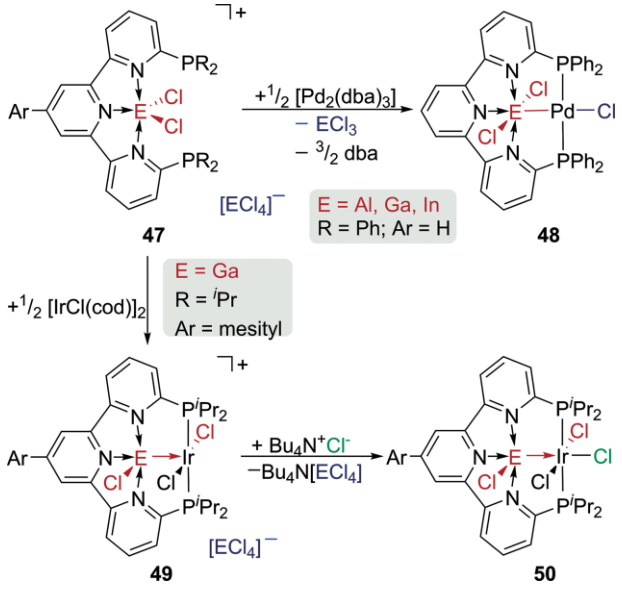

Scheme 18. Reactivity of group 13-based metallo-ligands towards different metal precursors, leading to different ligand types.

Neutral Lewis-Basic Metallo-Ligands

The reaction of the pre-ligand **47** with half an equivalent of $[IrCl(cod)]_2$ results in the formation of a different ligand type with respect to complexes derived from the $[Pd_2(dba)_3]$ precursor. In this case the $[ECl_4]^-$ counterion does not interact with the metal center and a chloride substituent migrates from the gallium to the iridium center upon coordination.[134] Formally, the formed complex **49** may be described as square pyramidal iridium(I) complex with a Lewis acidic cationic gallium(III)-based ligand or as iridium(III) complex with a gallylene-based donor group. Strong evidence for the latter interpretation is provided by the reaction with a chloride ion source such as Bu_4NCl, which leads to the coordination of a chloride ligand to the iridium center rather than to the gallium atom. Whereas the coordination to the gallium would lead to the ligand as observed for Pd complex **48**, formally categorized as X-type, the ligand in complex **50** is rather described as neutral L-type ligand.

In general, higher coordination numbers are put into effect with the heavier homologues serving as metallo-ligands. Moreover, the dissociation or migration of anionic substituents can be observed for all ligand types, leading to a change of the formal ligand type or cleavage of the metal ligand bond.

3.2. Metal-Based Pincer-Type Ligands Beyond a Distinct CBC Scheme

Emslie and co-workers reported a notable example of an PPM metallo-pincer ligand characterized by an aryldimethylalane moiety ("Me_2Al-arm") attached to an 1,1′-bis(phosphino)ferrocene unit. The ligand was employed in a series of Pt complexes of which the carbonyl complex [Pt(CO)(PPAl)] (**51**) drew our attention due to an notable bonding interaction with respect to alane coordination (Figure 9-I).[135] The crystal structure of **51** reveals a distorted square-planar coordination sphere around the Pt center built by the tridentate **[PPAl]** pincer and an ancillary CO ligand. While the CO ligand is located in the P–Pt–P plane the Al is significantly displaced out of this plane by more than 1 Å. The angle defined by C–Pt–Al is small (73.0(2)°) and, correspondingly, a short Al–C_{CO} interatomic distance (2.736(8) Å) is revealed indicating an additional bonding interaction between the Al metallo ligand and the CO ligand. The authors present bond order analysis of **51** and suitable model compounds. The interpretation by the authors involves a description of the Pt–Al–*C*O interaction as a multi-center bonding situation, where the electrons involved in σ-donation and π-backdonation of the Pt–CO carbonyl bonding are also involved in bonding to the alane. This multi-center bonding motif may contribute to the extraordinary robust alane coordination as the authors did neither observe hemilabile Al-coordination modes nor Al–C bond cleavage in a variety of complexes with Pt in different oxidation states and coordination geometries.

Similar additional ancillary ligand interactions in a silver complex with the bis-metallo-ligand $[(CO)_4Fe\text{-}N\text{-}Fe(CO)_4]$ (**54**, Figure 6-II) were reported by Mak and co-workers 20 years ago.[136] The ligand was prepared via the reaction of the pre-ligand 2,6-bis(diphenylphosphino)pyridine (**52**) and excess $[Fe(CO)_5]$ under concomitant loss of CO and Fe–P bond formation. Both iron centers in **53** reside a trigonal bipyramidal geometry with three CO ligands in equatorial position. Subsequent reaction with $AgClO_4$ gives rise to $[(Fe(CO)_4)_2((Ph_2P)_2py)Ag)]ClO_4$ (**54**,

© 2020 The Authors. European Journal of Inorganic Chemistry published by Wiley-VCH GmbH

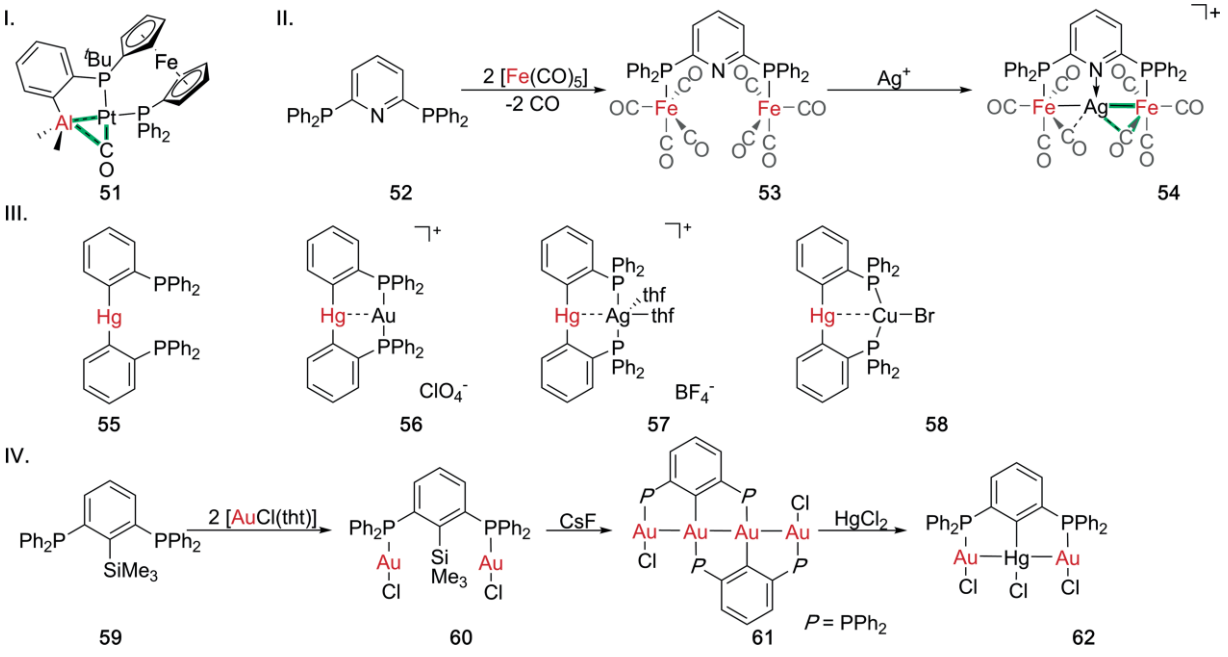

Figure 9. Synthesis of metallo-pincer-type complexes with unusual M–M bonding situations.

Figure 9-II). The silver center is chelated via the N donor of the pyridine and by two flanking $Fe(CO)_4$ groups ("iron arms") in a pincer-typical meridional fashion. The crystal structure displays the three metal centers Fe–Ag–Fe in an almost co-linear arrangement (ca. 171°) with Ag–Fe interatomic distances of 2.63 Å and 2.65 Å. The two Fe–Ag–N angles are approx. 90°. Both iron centers reside in a distorted octahedral geometry built by three CO ligands and the silver atom in equatorial position. The interaction of the silver center with the "Fe-arms" are further extended to an ancillary CO ligand of each $Fe(CO)_4$ moiety indicated by short interatomic Ag–C_{CO} distances of approx. 2.63 Å and 2.65 Å. The potential multi-center bonding situation was not further assessed by computations. The two examples above point to additional ancillary ligand interactions as intriguing features, which may have implications for a metallo-ligand design providing robust pincer-like chelation beyond an unequivocal CBC classification.

The following example shall illustrate unusual metallo pincer-like chelation involving metal–metal non-covalent interactions in the absence of secondary ligand interactions: Benett and co-workers reported the ligand bis{(2-diphenylphosphino)phenyl}mercury (**55,** Figure 9-III**).** Upon coordination of **55** to group 10 metals the authors noted short Hg–M interatomic distances and structural evidence was given for meridional P–Hg–P chelation.[137,138]

A study by López-de-Luzuriaga and co-workers involved **55** as tridentate chelate in coinage metal complexes (**56–58**, Figure 9-III)**.** The authors describe a straightforward reaction of the ligand and the corresponding metal salts to give compounds **56–58** featuring a L-M-L metallo-pincer motif. **55** offers a large P–P bite angle allowing for mutual *transoid*-coordination and thus leaving the central Hg atom in close vicinity to the transition metal center. The molecular structures of all complexes **56–58** derived from an XRD study show similar P–Hg–P metallo-pincer-type bonding features, characterized by linearly coordinated Hg via two phenylates and short Hg–M (M = Au, Ag, Cu) interatomic distances (2.9194(7) Å **56**, 3.0544(2) Å **57**, 2.8656(5) Å **58**). The Au metal center in **56**, resides in a distorted T-shape array. The Ag center in **57** is additionally coordinated by two THF solvent molecules in equatorial and apical position giving rise to a rather square pyramidal geometry. The counter anions in both compounds exhibit weak interactions with the Hg center. The copper center in compound **58** resides in a trigonal pyramidal structure built by the two P-donors and the bromide ligand with the Hg center remaining in apical position. The authors analyzed the Hg–M interactions by means of ab initio calculations on suitable model compounds and concluded for all compounds similar metallophilic interactions originating from dispersive forces.[139] Note, the above mentioned dinuclear metal complexes, obviously, can also be described as Hg complexes with dianionic (bisphenylate) [X–M–X] (M = Au, Ag; Cu) pincer ligand. However, with respect to the synthesis strategy i.e. the initial preparation of **55**, we prefer to describe them as complexes with L–Hg–L metallo-pincer-ligand.

Closed-shell metallophilic interactions were also suggested for related complexes with tridentate ligand-structures involving 6-diphenylpholphinoacenaph-5-yl-mercury (Hg–Au/Ag/Cu).[140,141]

We have recently prepared the anionic bisphosphino-phenylate ligand $[2,6\text{-}(Ph_2P)C_6H_3]^-$ (**PCP**, Figure 9-IV), which is a potent pre-ligand for an anionic AuC^-Au metallo pincer ligand. **PCP** is isoelectronic to 2,6-bis(diphenylphosphino)pyridine (**52**) and provides a rigid scaffold due to direct 2,6-substitution of the central phenyl ring. Several multi-core complexes were prepared in which **PCP** hosts tetra-nuclear Au_4- strings (e.g. **61** in Figure 9-IV) and route-like structures,[142] as well as a Cu_4 dis-

© 2020 The Authors. European Journal of Inorganic Chemistry published by Wiley-VCH GmbH

torted rhombic arrangement,[143] all showing close M–M interactions.

The synthesis of the hetero-bimetallic tri-nuclear "metallo-pincer-type" complex **62** involved a mild stepwise approach: Firstly, two equiv. [AuCl(tht)] (tht = tetrahydrothiophene) were treated with the ligand precursor [2,6-(Ph_2P)C_6H_3($SiMe_3$)] (**59**) to give [Au–$CSiMe_3$–Au] (**60,** Figure 9-IV**)**, where each of the two Au centers are coordinated by a P-donor of **59** and a chlorido ligand in a linear geometry. Subsequent addition of CsF gave rise to Me_3Si–C bond cleavage and formation of the organometallic Au_4 string complex (**61**, Figure 9-IV). In this pathway -$SiMe_3$ serves as a suitable protective group for the phenylate carbon donor. Eventually, addition of $HgCl_2$ gave the "metallo-pincer" complex **62** (Figure 9-IV).

Single crystal XRD structural analysis disclosed the [Au–C^-–Au] ligand in **62** to provide M–X–M meridional pincer-type chelation via the central carbanionic binding site and two Au–Hg interactions. Two conformers of complex **62** were found, in which the two flanking Au atoms bind to the Hg center either in mutual *cisoid* and *transoid* arrangement. The Au–Hg interatomic distances ranging from approx. 3.03–3.41 Å. The distorted planar coordination sphere of the Hg^{II} center in both conformers is completed by a chlorido ligand. In contrast to complex **51** and **54** there are no ancillary co-ligand interactions evident e.g. Hg–Cl–Au interactions. Computational evaluation of electronic bond characteristics of the Au–Hg–Au string using real-space bond indicators derived from electron density methods (AIM, ELI-D, NCI) suggested non-covalent metallophilic interactions between the Au and the Hg centers in **62**, as well as for the Au–Au interactions in the string compound **61.**

It was demonstrated that non-covalent interactions can shape pincer-type ligand motifs, as shown for complex **62**. The findings may suggest considering non-covalent interactions as intriguing bonding features in metallo-pincer complexes, exceeding a common CBC grouping of the metallo-ligand interaction.

4. Conclusion

In summary, we attempt to demonstrate that a broad range of different bonding interactions can lead to stable arrangements, in pincer-type ligation motifs. In particular ligating groups which are based on group 13 elements were reported to exhibit unusual properties in recent years. Especially, for the heavier homologues acting as metallo ligands, the classification according to the CBC can be challenging. In this context, we highlighted that interactions other than the covalent interactions defined in the CBC can lead to stable pincer-type complexes and that the current view might be extended.

Acknowledgments

We gratefully acknowledge financial support from the Deutsche Forschungsgemeinschaft (LA 2830/6-1), for funding R. L. within the Heisenberg-program (LA 2830/8-1). Open access funding enabled and organized by Projekt DEAL.

Keywords: Pincer ligands · Metal-ligand interactions · Metal-metal interactions · Cooperative effects · Ligand design

[1] *The Privileged Pincer-Metal Platform: Coordination Chemistry & Applications* (Eds. G. van Koten, R. A. Gossage), Springer International Publishing, **2016**.
[2] E. Peris, R. H. Crabtree, *Chem. Soc. Rev.* **2018**, *47*, 1959–1968.
[3] C. Gunanathan, D. Milstein, *Chem. Rev.* **2014**, *114*, 12024–12087.
[4] H. Valdés, M. A. García-Eleno, D. Canseco-Gonzalez, D. Morales-Morales, *ChemCatChem* **2018**, *10*, 3136–3172.
[5] L. S. Merz, J. Ballmann, L. H. Gade, *Eur. J. Inorg. Chem.* **2020**, *2020*, 1–21.
[6] L. Alig, M. Fritz, S. Schneider, *Chem. Rev.* **2019**, *119*, 2681–2751.
[7] S. Schneider, J. Meiners, B. Askevold, *Eur. J. Inorg. Chem.* **2012**, *2012*, 412–429.
[8] J. R. Khusnutdinova, D. Milstein, *Angew. Chem. Int. Ed.* **2015**, *54*, 12236–12273; *Angew. Chem.* **2015**, *127*, 12406.
[9] C. Gunanathan, D. Milstein, *Acc. Chem. Res.* **2011**, *44*, 588–602.
[10] A. Singh, D. Gelman, *ACS Catal.* **2020**, *10*, 1246–1255.
[11] M. Gozin, M. Aizenberg, S.-Y. Liou, A. Weisman, Y. Ben-David, D. Milstein, *Nature* **1994**, *370*, 42–44.
[12] W. H. Bernskoetter, C. K. Schauer, K. I. Goldberg, M. Brookhart, *Science* **2009**, *326*, 553–556.
[13] A. Nerush, M. Vogt, U. Gellrich, G. Leitus, Y. Ben-David, D. Milstein, *J. Am. Chem. Soc.* **2016**, *138*, 6985–6997.
[14] B. Guo, D. S. Zijlstra, J. G. de Vries, E. Otten, *ChemCatChem* **2018**, *10*, 2868–2872.
[15] C. J. Moulton, B. L. Shaw, *J. Chem. Soc., Dalton Trans.* **1976**, 1020–1024.
[16] G. van Koten, K. Timmer, J. G. Noltes, A. L. Spek, *J. Chem. Soc., Chem. Commun.* **1978**, *045*, 250–252.
[17] G. van Koten, *Pure Appl. Chem.* **1989**, *61*, 1681–1694.
[18] See ref.[2].
[19] M. L. H. Green, G. Parkin, *Dalton Trans.* **2016**, *45*, 18784–18795.
[20] M. L. H. Green, *J. Organomet. Chem.* **1995**, *500*, 127–148.
[21] M. L. H. Green, G. Parkin, *J. Chem. Educ.* **2014**, *91*, 807–816.
[22] J. S. Jones, C. R. Wade, M. Yang, F. P. Gabbaï, *Dalton Trans.* **2017**, *46*, 5598–5604.
[23] J. S. Jones, F. P. Gabbaï, *Acc. Chem. Res.* **2016**, *49*, 857–867.
[24] D. You, H. Yang, S. Sen, F. P. Gabbaï, *J. Am. Chem. Soc.* **2018**, *140*, 9644–9651.
[25] D. You, F. P. Gabbaï, *Trends Chem.* **2019**, *1*, 485–496.
[26] K. W. Muir, J. A. Ibers, *Inorg. Chem.* **1969**, *8*, 1921–1928.
[27] A. F. Hill, G. R. Owen, A. J. White, D. J. Williams, *Angew. Chem. Int. Ed.* **1999**, *38*, 2759–2761; *Angew. Chem.* **1999**, *111*, 2920.
[28] S. Bontemps, H. Gornitzka, G. Bouhadir, K. Miqueu, D. Bourissou, *Angew. Chem. Int. Ed.* **2006**, *45*, 1611–1614; *Angew. Chem.* **2006**, *118*, 1641.
[29] M. Sircoglou, S. Bontemps, M. Mercy, N. Saffon, M. Takahashi, G. Bouhadir, L. Maron, D. Bourissou, *Angew. Chem. Int. Ed.* **2007**, *46*, 8583–8586; *Angew. Chem.* **2007**, *119*, 8737.
[30] A. Amgoune, D. Bourissou, *Chem. Commun.* **2011**, *47*, 859–871.
[31] I. R. Crossley, A. F. Hill, A. C. Willis, *Organometallics* **2010**, *29*, 326–336.
[32] A. F. Hill, S. B. Lee, J. Park, R. Shang, A. C. Willis, *Organometallics* **2010**, *29*, 5661–5669.
[33] I. R. Crossley, A. F. Hill, A. C. Willis, *Organometallics* **2005**, *24*, 1062–1064.
[34] W. H. Harman, J. C. Peters, *J. Am. Chem. Soc.* **2012**, *134*, 5080–5082.
[35] P. Steinhoff, M. E. Tauchert, *Beilstein J. Org. Chem.* **2016**, *12*, 1573–1576.
[36] H. Fong, M. E. Moret, Y. Lee, J. C. Peters, *Organometallics* **2013**, *32*, 3053–3062.
[37] D. L. M. Suess, J. C. Peters, *J. Am. Chem. Soc.* **2013**, *135*, 4938–4941.
[38] S. N. MacMillan, W. Hill Harman, J. C. Peters, *Chem. Sci.* **2014**, *5*, 590–597.
[39] W. H. Harman, T. P. Lin, J. C. Peters, *Angew. Chem. Int. Ed.* **2014**, *53*, 1081–1086; *Angew. Chem.* **2014**, *126*, 1099.
[40] T. Schindler, M. Lux, M. Peters, L. T. Scharf, H. Osseili, L. Maron, M. E. Tauchert, *Organometallics* **2015**, *34*, 1978–1984.
[41] M. A. Nesbit, D. L. M. Suess, J. C. Peters, *Organometallics* **2015**, *34*, 4741–4752.
[42] W.-C. Shih, W. Gu, M. C. MacInnis, S. D. Timpa, N. Bhuvanesh, J. Zhou, O. V. Ozerov, *J. Am. Chem. Soc.* **2016**, *138*, 2086–2089.

© 2020 The Authors. European Journal of Inorganic Chemistry published by Wiley-VCH GmbH

[43] F. Inagaki, C. Matsumoto, Y. Okada, N. Maruyama, C. Mukai, *Angew. Chem. Int. Ed.* **2015**, *54*, 818–822; *Angew. Chem.* **2015**, *127*, 832.
[44] G. Bouhadir, D. Bourissou, *Chem. Soc. Rev.* **2016**, *45*, 1065–1079.
[45] H. Kameo, J. Yamamoto, A. Asada, H. Nakazawa, H. Matsuzaka, D. Bourissou, *Angew. Chem. Int. Ed.* **2019**, *58*, 18783–18787; *Angew. Chem.* **2019**, *131*, 18959–18963.
[46] D. J. H. Emslie, B. E. Cowie, K. B. Kolpin, *Dalton Trans.* **2012**, *41*, 1101–1117.
[47] Y. Li, C. Hou, J. Jiang, Z. Zhang, C. Zhao, A. J. Page, Z. Ke, *ACS Catal.* **2016**, *6*, 1655–1662.
[48] Y. Li, J. Liu, X. Huang, L. B. Qu, C. Zhao, R. Langer, Z. Ke, *Chem. Eur. J.* **2019**, *25*, 13785–13798.
[49] M. E. O'Reilly, A. S. Veige, *Chem. Soc. Rev.* **2014**, *43*, 6325–6369.
[50] S. S. Nadif, T. Kubo, S. A. Gonsales, S. VenkatRamani, I. Ghiviriga, B. S. Sumerlin, A. S. Veige, *J. Am. Chem. Soc.* **2016**, *138*, 6408–6411.
[51] C. D. Roland, H. Li, K. A. Abboud, K. B. Wagener, A. S. Veige, *Nat. Chem.* **2016**, *8*, 791–796.
[52] Y. Segawa, M. Yamashita, K. Nozaki, *Science* **2006**, *314*, 113–115.
[53] Y. Segawa, M. Yamashita, K. Nozaki, *Organometallics* **2009**, *28*, 6234–6242.
[54] Y. Segawa, M. Yamashita, K. Nozaki, *J. Am. Chem. Soc.* **2009**, *131*, 9201–9203.
[55] H. Ogawa, M. Yamashita, *Dalton Trans.* **2013**, *42*, 625–629.
[56] K. Tanoue, M. Yamashita, *Organometallics* **2015**, *34*, 4011–4017.
[57] E. H. Kwan, H. Ogawa, M. Yamashita, *ChemCatChem* **2017**, *9*, 2457–2462.
[58] E. H. Kwan, Y. J. Kawai, S. Kamakura, M. Yamashita, *Dalton Trans.* **2016**, *45*, 15931–15941.
[59] M. Hasegawa, Y. Segawa, M. Yamashita, K. Nozaki, *Angew. Chem. Int. Ed.* **2012**, *51*, 6956–6960; *Angew. Chem.* **2012**, *124*, 7062.
[60] M. Yamashita, *Bull. Chem. Soc. Jpn.* **2016**, *89*, 269–281.
[61] T.-P. Lin, J. C. Peters, *J. Am. Chem. Soc.* **2013**, *135*, 15310–15313.
[62] G. Ganguly, T. Malakar, A. Paul, *ACS Catal.* **2015**, *5*, 2754–2769.
[63] D. Schuhknecht, F. Ritter, M. E. Tauchert, *Chem. Commun.* **2016**, *52*, 11823–11826.
[64] P. Ríos, A. Rodríguez, J. López-Serrano, *ACS Catal.* **2016**, *6*, 5715–5723.
[65] Y. Li, J. Liu, C. Hou, Y. Shao, L. B. Qu, C. Zhao, Z. Ke, *Catal. Sci. Technol.* **2018**, *8*, 3395–3405.
[66] M. F. Silva Valverde, P. Schweyen, D. Gisinger, T. Bannenberg, M. Freytag, C. Kleeberg, M. Tamm, *Angew. Chem. Int. Ed.* **2017**, *56*, 1135–1140; *Angew. Chem.* **2017**, *129*, 1155.
[67] A. J. Rosenthal, S. Mallet-Ladeira, G. Bouhadir, E. D. Sosa-Carrizo, K. Miqueu, D. Bourissou, *Organometallics* **2018**, *37*, 755–760.
[68] P. Bissinger, H. Braunschweig, A. Damme, I. Krummenacher, A. K. Phukan, K. Radacki, S. Sugawara, *Angew. Chem. Int. Ed.* **2014**, *53*, 7360–7363; *Angew. Chem.* **2014**, *126*, 7488.
[69] F. Dahcheh, D. Martin, D. W. Stephan, G. Bertrand, *Angew. Chem. Int. Ed.* **2014**, *53*, 13159–13163; *Angew. Chem.* **2014**, *126*, 13375.
[70] A. J. Rosenthal, M. Devillard, K. Miqueu, G. Bouhadir, D. Bourissou, *Angew. Chem. Int. Ed.* **2015**, *54*, 9198–9202; *Angew. Chem.* **2015**, *127*, 9330.
[71] S. H. Ueng, A. Solovyev, X. Yuan, S. J. Geib, L. Fensterbank, E. Lacôte, M. Malacria, M. Newcomb, J. C. Walton, D. P. Curran, *J. Am. Chem. Soc.* **2009**, *131*, 11256–11262.
[72] J. C. Walton, M. M. Brahmi, L. Fensterbank, E. Lacôte, M. Malacria, Q. Chu, S. H. Ueng, A. Solovyev, D. P. Curran, *J. Am. Chem. Soc.* **2010**, *132*, 2350–2358.
[73] T. Matsumoto, F. P. Gabbai, *Organometallics* **2009**, *28*, 4252–4253.
[74] H. Braunschweig, R. D. Dewhurst, F. Hupp, M. Nutz, K. Radacki, C. W. Tate, A. Vargas, Q. Ye, *Nature* **2015**, *522*, 327–330.
[75] L. Kong, Y. Li, R. Ganguly, D. Vidovic, R. Kinjo, *Angew. Chem. Int. Ed.* **2014**, *53*, 9280–9283; *Angew. Chem.* **2014**, *126*, 9434.
[76] R. Kinjo, B. Donnadieu, M. A. Celik, G. Frenking, G. Bertrand, *Science* **2011**, *333*, 610–613.
[77] M. A. Celik, R. Sure, S. Klein, R. Kinjo, G. Bertrand, G. Frenking, *Chem. Eur. J.* **2012**, *18*, 5676–5692.
[78] L. Vondung, N. Frank, M. Fritz, L. Alig, R. Langer, *Angew. Chem. Int. Ed.* **2016**, *55*, 14450–14454; *Angew. Chem.* **2016**, *128*, 14665.
[79] L. Maser, L. Vondung, R. Langer, *Polyhedron* **2018**, *143*, 28–42.
[80] M. Grätz, A. Bäcker, L. Vondung, L. Maser, A. Reincke, R. Langer, *Chem. Commun.* **2017**, *53*, 7230–7233.
[81] L. Maser, C. Schneider, L. Alig, R. Langer, *Inorganics* **2019**, *7*, 61.
[82] L. Maser, C. Schneider, L. Vondung, L. Alig, R. Langer, *J. Am. Chem. Soc.* **2019**, *141*, 7596–7604.
[83] A. Bäcker, Y. Li, M. Fritz, M. Grätz, Z. Ke, R. Langer, *ACS Catal.* **2019**, *9*, 7300–7309.
[84] L. Vondung, P. Jerabek, R. Langer, *Chem. Eur. J.* **2019**, *25*, 3068–3076.
[85] H. Li, C. C. C. Johansson Seechurn, T. J. Colacot, *ACS Catal.* **2012**, *2*, 1147–1164.
[86] R. Martin, S. L. Buchwald, *Acc. Chem. Res.* **2008**, *41*, 1461–1473.
[87] A. F. Littke, G. C. Fu, *Angew. Chem. Int. Ed.* **2002**, *41*, 4176–4211; *Angew. Chem.* **2002**, *114*, 4350.
[88] A. Zapf, M. Beller, *Chem. Commun.* **2005**, 431–440.
[89] R. H. Grubbs, *Angew. Chem. Int. Ed.* **2006**, *45*, 3760–3765; *Angew. Chem.* **2006**, *118*, 3845.
[90] J. Tappen, I. Rodstein, K. McGuire, A. Großjohann, J. Löffler, T. Scherpf, V. H. Gessner, *Chem. Eur. J.* **2020**, *26*, 4281–4288.
[91] P. Weber, T. Scherpf, I. Rodstein, D. Lichte, L. T. Scharf, L. J. Gooßen, V. H. Gessner, *Angew. Chem. Int. Ed.* **2019**, *58*, 3203–3207; *Angew. Chem.* **2019**, *131*, 3235.
[92] M. A. Wünsche, P. Mehlmann, T. Witteler, F. Buß, P. Rathmann, F. Dielmann, *Angew. Chem. Int. Ed.* **2015**, *54*, 11857–11860; *Angew. Chem.* **2015**, *127*, 12024–12027.
[93] L. T. Scharf, I. Rodstein, M. Schmidt, T. Scherpf, V. H. Gessner, *ACS Catal.* **2020**, *10*, 999–1009.
[94] O. V. Ozerov, C. Guo, V. A. Papkov, B. M. Foxman, *J. Am. Chem. Soc.* **2004**, *126*, 4792–4793.
[95] R. J. Errington, W. S. McDonald, B. L. Shaw, *J. Chem. Soc., Dalton Trans.* **1982**, *2*, 1829–1835.
[96] H. D. Empsall, E. M. Hyde, R. Markham, W. S. McDonald, M. C. Norton, B. L. Shaw, B. Weeks, *J. Chem. Soc., Chem. Commun.* **1977**, *006*, 589.
[97] D. G. Gusev, A. J. Lough, *Organometallics* **2002**, *21*, 2601–2603.
[98] P. Paetzold, U. Englert, R. Finger, T. Schmitz, A. Tapper, R. Ziembinski, *Z. Anorg. Allg. Chem.* **2004**, *630*, 508–518.
[99] A. Iannetelli, R. C. Da Costa, A. J. Guwy, G. J. Tizzard, S. J. Coles, G. R. Owen, *Organometallics* **2020**, *39*, 1976–1988.
[100] C. Defieber, H. Grützmacher, E. M. Carreira, *Angew. Chem. Int. Ed.* **2008**, *47*, 4482–4502; *Angew. Chem.* **2008**, *120*, 4558.
[101] D. G. A. Verhoeven, M.-E. Moret, *Dalton Trans.* **2016**, *45*, 15762–15778.
[102] M. J. S. Dewar, G. P. Ford, *J. Am. Chem. Soc.* **1979**, *101*, 783–791.
[103] G. Vasapollo, A. Sacco, C. F. Nobile, M. A. Pellinghelli, M. Lanfranchi, *J. Organomet. Chem.* **1986**, *312*, 249–262.
[104] G. Vasapollo, C. F. Nobile, M. Latronico, M. Lanfranchi, M. A. Pellinghelli, *J. Organomet. Chem.* **1987**, *336*, 429–439.
[105] M. A. Bennett, R. N. Johnson, I. B. Tomkins, *J. Organomet. Chem.* **1976**, *118*, 205–232.
[106] M. A. Bennett, P. W. Clark, *J. Organomet. Chem.* **1976**, *110*, 367–381.
[107] M. Bennett, S. Corlett, G. Robertson, W. Steffen, *Aust. J. Chem.* **1980**, *33*, 1261.
[108] B. J. Barrett, V. M. Iluc, *Organometallics* **2014**, *33*, 2565–2574.
[109] B. J. Barrett, V. M. Iluc, *Inorg. Chim. Acta* **2017**, *460*, 35–42.
[110] B. J. Barrett, V. M. Iluc, *Inorg. Chem.* **2014**, *53*, 7248–7259.
[111] K. Okamoto, Y. Omoto, H. Sano, K. Ohe, *Dalton Trans.* **2012**, *41*, 10926.
[112] K. Sasakura, K. Okamoto, K. Ohe, *Organometallics* **2018**, *37*, 2319–2324.
[113] N. J. Greco, M. Hysell, J. R. Goldenberg, A. L. Rheingold, Y. Tor, *Dalton Trans.* **2006**, 2288.
[114] P. Federmann, T. Richter, H. Wadepohl, J. Ballmann, *Organometallics* **2019**, *38*, 4307–4318.
[115] J. A. Buss, T. Agapie, *Nature* **2016**, *529*, 72–75.
[116] J. A. Buss, G. A. Edouard, C. Cheng, J. Shi, T. Agapie, *J. Am. Chem. Soc.* **2014**, *136*, 11272–11275.
[117] J. A. Buss, G. A. Bailey, J. Oppenheim, D. G. VanderVelde, W. A. Goddard, T. Agapie, *J. Am. Chem. Soc.* **2019**, *141*, 15664–15674.
[118] See ref.[8].
[119] J. I. van der Vlugt, J. N. H. Reek, *Angew. Chem. Int. Ed.* **2009**, *48*, 8832–8846; *Angew. Chem.* **2009**, *121*, 8990.
[120] C. A. Huff, J. W. Kampf, M. S. Sanford, *Organometallics* **2012**, *31*, 4643–4645.
[121] M. Vogt, A. Nerush, Y. Diskin-Posner, Y. Ben-David, D. Milstein, *Chem. Sci.* **2014**, *5*, 2043–2051.
[122] M. Vogt, M. Gargir, M. A. Iron, Y. Diskin-Posner, Y. Ben-David, D. Milstein, *Chem. Eur. J.* **2012**, *18*, 9194–9197.

© 2020 The Authors. European Journal of Inorganic Chemistry published by Wiley-VCH GmbH

[123] A. Kumar, P. Daw, N. A. Espinosa-Jalapa, G. Leitus, L. J. W. Shimon, Y. Ben-David, D. Milstein, *Dalton Trans.* **2019**, *48*, 14580–14584.
[124] G. A. Filonenko, M. P. Conley, C. Copéret, M. Lutz, E. J. M. Hensen, E. A. Pidko, *ACS Catal.* **2013**, *3*, 2522–2526.
[125] I. Heuermann, B. Heitmann, R. Stichauer, D. Duvinage, M. Vogt, *Organometallics* **2019**, *38*, 1787–1799.
[126] M. Sircoglou, G. Bouhadir, N. Saffon, K. Miqueu, D. Bourissou, *Organometallics* **2008**, *27*, 1675–1678.
[127] M. Sircoglou, M. Mercy, N. Saffon, Y. Coppel, G. Bouhadir, L. Maron, D. Bourissou, *Angew. Chem. Int. Ed.* **2009**, *48*, 3454–3457; *Angew. Chem.* **2009**, *121*, 3506.
[128] P. Steinhoff, R. Steinbock, A. Friedrich, B. G. Schieweck, C. Cremer, K.-N. Truong, M. E. Tauchert, *Dalton Trans.* **2018**, *47*, 10439–10442.
[129] P. Steinhoff, M. Paul, J. P. Schroers, M. E. Tauchert, *Dalton Trans.* **2019**, *48*, 1017–1022.
[130] K. Semba, I. Fujii, Y. Nakao, *Inorganics* **2019**, *7*, 140.
[131] N. Hara, T. Saito, K. Semba, N. Kuriakose, H. Zheng, S. Sakaki, Y. Nakao, *J. Am. Chem. Soc.* **2018**, *140*, 7070–7073.
[132] S. Morisako, S. Watanabe, S. Ikemoto, S. Muratsugu, M. Tada, M. Yamashita, *Angew. Chem. Int. Ed.* **2019**, *58*, 15031; *Angew. Chem.* **2019**, *131*, 15173–15177.
[133] J. Takaya, N. Iwasawa, *J. Am. Chem. Soc.* **2017**, *139*, 6074–6077.
[134] N. Saito, J. Takaya, N. Iwasawa, *Angew. Chem. Int. Ed.* **2019**, *58*, 9998–10002; *Angew. Chem.* **2019**, *131*, 10103.
[135] B. E. Cowie, F. A. Tsao, D. J. H. Emslie, *Angew. Chem. Int. Ed.* **2015**, *54*, 2165–2169; *Angew. Chem.* **2015**, *127*, 2193.
[136] H.-B. Song, Z.-Z. Zhang, T. C. W. Mak, *Inorg. Chem.* **2001**, *40*, 5928–5933.
[137] M. A. Bennett, M. Contel, D. C. R. Hockless, L. L. Welling, *Chem. Commun.* **1998**, 2401–2402.
[138] M. A. Bennett, M. Contel, D. C. R. Hockless, L. L. Welling, A. C. Willis, *Inorg. Chem.* **2002**, *41*, 844–855.
[139] J. M. López-de-Luzuriaga, M. Monge, M. E. Olmos, D. Pascual, *Organometallics* **2015**, *34*, 3029–3038.
[140] E. Hupf, E. Lork, S. Mebs, J. Beckmann, *Inorg. Chem.* **2015**, *54*, 1847–1859.
[141] E. Hupf, R. Kather, M. Vogt, E. Lork, S. Mebs, J. Beckmann, *Inorg. Chem.* **2016**, *55*, 11513–11521.
[142] M. Olaru, J. F. Kögel, R. Aoki, R. Sakamoto, H. Nishihara, E. Lork, S. Mebs, M. Vogt, J. Beckmann, *Chem. Eur. J.* **2020**, *26*, 275–284.
[143] M. Olaru, E. Rychagova, S. Ketkov, Y. Shynkarenko, S. Yakunin, M. V. Kovalenko, A. Yablonskiy, B. Andreev, F. Kleemiss, J. Beckmann, M. Vogt, *J. Am. Chem. Soc.* **2020**, *142*, 373–381.

Received: May 27, 2020

© 2020 The Authors. European Journal of Inorganic Chemistry published by Wiley-VCH GmbH